Single-Column Simulated-Moving-Bed Process with Recycle Lag

José P. B. Mota and João M. M. Araújo
Requimte/CQFB, Depto. de Química, Faculdade de Ciências e Tecnologia, Universidade Nova de Lisboa, 2829-516 Caparica, Portugal

DOI 10.1002/aic.10426
Published online April 27, 2005 in Wiley InterScience (www.interscience.wiley.com).

It is shown that the periodic state of the simulated-moving-bed (SMB) process is reproduced by a single-column chromatographic process with a recycle lag of $(N - 1)\tau$ time units, where N is the number of columns of the equivalent SMB unit and τ is the switching time. The operation of this ideal single-column process is formulated by selecting an arbitrary column of the SMB and following its operation over a complete cycle. To implement the recycle lag in practice, a special type of plug-flow tube has been designed. It includes internal elements to make the flow as close as possible to plug flow, and a piston to compensate for the difference between the inlet and outlet flow rates. This is necessary because the recycle lag is not a multiple of the overall cycle duration. The proposed system is a more compact, less-expensive, and simpler-to-operate alternative to the SMB. It avoids the problem of packing reproducibility and the total pressure drop is 1/Nth of that of the equivalent SMB. Depending on the efficiency of the recycle tube, our single-column process can achieve the same purities as the analogous SMB unit while keeping the specific productivity constant. © 2005 American Institute of Chemical Engineers
AIChE J, 51: 1641–1653, 2005
Keywords: single-column process, analogue, chromatography (LC & SMB), chromatography (preparative)

Introduction

Simulated-moving-bed (SMB) chromatography has been increasingly applied for the separation of pure substances in the pharmaceutical, fine chemistry, and biotechnology industries, at all production scales, from laboratory to pilot to production scale.[1] The SMB has many advantages with respect to discontinuous batch chromatography,[2] such as higher product purity, less solvent consumption, and higher productivity per unit stationary phase.[3-5]

Thanks to recent developments in cyclic operation policies, a number of possibilities for improving SMB performance have emerged through variation of parameters during a switching interval. These include, among others, the nonsynchronous shift of the inlet and outlet ports within a global switching period,[6] modulation of solvent strength during process operation,[7] and cyclic modulation of feed flow[8,9] and feed concentration.[10] These advances are pushing the trend toward the use of units with smaller number of columns[11-13] because less stationary phase is used and the setup is more economical.[14]

In many cases it would be advantageous to work with the limiting case of a single-column. Because only one column would have to be repacked, switching from one mixture to another would be easier and take less time than with an SMB. This is especially important for the pharmaceutical industry, where SMBs are seen as multipurpose units that can be applied to different separations in all stages of the drug-development cycle.[1]

In this line of work, Abunasser et al.[15] recently developed a one-column chromatographic process with recycle analogous to a four-section SMB, which they termed "the analog." The analog has one chromatographic column connected to a num-

Correspondence concerning this article should be addressed to J. P. B. Mota at pmota@dq.fct.unl.pt.

Table 1. Operating Conditions and Model Parameters for the Separation of Binaphthol Enantiomers by SMB Chromatography on Cellulose Triacetate Using Heptane–Isopropanol (72:28) as Eluent[17]

Adsorption Equilibrium Isotherms

$$(q_A^*, q_B^*) = \frac{(2.69c_A, 3.73c_B)}{1 + 0.0336c_A + 0.0466c_B} + \frac{(0.1c_A, 0.3c_B)}{1 + c_A + 3c_B}$$

Feed flow rate	$Q_F = 3.64$ mL/min	Porosity ratio	$\phi = 1.5$
Eluent flow rate	$Q_E = 21.45$ mL/min	Column diameter	$d = 2.6$ cm
Raffinate flow rate	$Q_R = 7.11$ mL/min	Péclet number	$\widetilde{Pe} = v_j L_j / D = 2000$
Extract flow rate	$Q_X = 17.98$ mL/min	LDF coefficients	$k_i = (0.1, 0.1)\ s^{-1}$
Recycle flow rate	$Q = 35.38$ mL/min	Feed concentration	$c_i^F = (2.9, 2.9)$ g/L
Zone length	$L_j N/4 = 21.0$ cm	Cycle duration	$N\tau = 24$ min

ber of tanks equal to the number of steps of the SMB cycle. These allow for recycling in a manner that mimics SMB operation. The analog and corresponding SMB were analyzed for the separation of dextran T6-fructose and dextran T6-raffinose mixtures and for the separation of binaphthol enantiomers. Because of mixing in the tanks, lower purities are obtained with the analog than with the SMB for the same productivity and eluent-to-feed (Q_E/Q_F) values. The purities can be increased either by dividing the tanks into several smaller ones or by increasing the Q_E/Q_F value.

In a subsequent work[16] both start-up and shutdown analyses were performed for the analog, which are particularly useful in short campaigns. The authors concluded that correct start-up conditions can reduce the time needed to reach steady state by 50%. Several strategies were suggested to reduce the time and amount of eluent used during shutdown. The concept of the one-column analog was also successfully applied to various three-zone SMB configurations and to the VARICOL® process.[6]

Inspired by the work of these authors we have developed a novel single-column SMB analog that uses a special type of plug-flow device to implement the appropriate recycle pattern for the process to mimic the corresponding SMB. We first derive the necessary conditions for a single-column chromatographic process to reproduce the periodic state of the SMB. This analysis leads to the concept of an *ideal* single-column analog, that is, a process that theoretically is indistinguishable from the equivalent SMB, except for the discontinuous use of the inlet/outlet lines. We then discuss how this process can be implemented in practice. Using an enantiomeric separation as a case study, the efficiency of our process is compared with that of the target SMB. For reference, the comparison is also extended to the analog developed by Wankat and coworkers.[15,16] We show that, depending on the efficiency of the recycle tube, our single-column process can achieve the same purities as those of the analogous SMB unit while keeping the specific productivity constant.

For brevity of presentation, a single case of enantiomeric separation is analyzed in this study, although the conclusions are of general applicability. The selected case study is the separation of binaphthol enantiomers,[17] carried out using cellulose triacetate as stationary phase and heptane–isopropanol (72:28) as eluent.[18,19] The adsorption equilibrium is well described by a bi-Langmuir competitive isotherm model. The operating conditions and model parameters for this chromatographic separation using SMB are listed in Table 1. The operating parameters have been optimized by Pais et al.[17] and provide a reasonably good separation.

Theoretical Basis for the Single-Column SMB Analog

We start by reviewing the mathematical basis of the SMB process because it is a prerequisite for the development and understanding of their single-column analogous processes. Only those aspects that are relevant to the present work are discussed here. More details can be found elsewhere.[20,21]

The classical SMB unit consists of N identical chromatographic columns that are interconnected circularly. By moving the input and withdrawal ports one column ahead (that is, in the direction of fluid flow) at fixed time intervals, the countercurrent contact between the adsorbent and liquid is simulated. The working principle of the SMB is illustrated in Figure 1. At each instant the active ports divide the columns into four sections, each playing a specific role in the separation. The binary mixture to be separated is fed between sections II and III, where the two components are separated. The more-retained species A and the less-retained species B are collected in the extract and raffinate streams, respectively. A desorbent or eluent is fed to section I to regenerate the solid before recycling and the fluid phase is regenerated in turn in section IV.

We assume that the isothermal operation of the chromato-

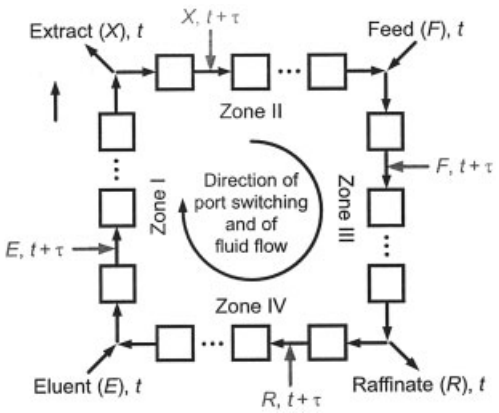

Figure 1. Scheme of the simulated moving bed process.

Several chromatographic columns are connected in a loop; the input and withdrawal ports are moved one column ahead every τ time units. The feed, eluent, extract, and raffinate streams are denoted by F, E, X, and R, respectively.

graphic columns can be adequately described by an axially dispersed flow model with finite mass-transfer rate described by a linear driving force (LDF) approximation. Although these assumptions are not strictly necessary for the discussion that follows, they provide a reasonably good description of a chromatographic column and were assumed to hold for the simulation results reported in this work. They are standard practice in SMB modeling.[22]

The solute material balance in a differential volume of column j ($j = 1, \ldots, N$) can be written as

$$\frac{\partial c_{ij}}{\partial t} + \phi \frac{\partial q_{ij}}{\partial t} = D_{ij} \frac{\partial^2 c_{ij}}{\partial z^2} - v_j \frac{\partial c_{ij}}{\partial z} \qquad (0 < z < L) \quad (1)$$

where $i = \mathrm{A}, \mathrm{B}$ identifies the species in the mixture, $\phi = (1 - \varepsilon)/\varepsilon$, ε is the bed porosity, L is the column length, c is the liquid-phase concentration, q is the adsorbed-phase concentration, v is the interstitial liquid velocity, and D is the axial dispersion coefficient.

The approximation of the adsorption rate by the LDF model leads to

$$\frac{\partial q_{ij}}{\partial t} = k_i (q_{ij}^* - q_{ij}) \qquad q_{ij}^* \equiv q_i^*(c_{\mathrm{A}j}, c_{\mathrm{B}j}) \qquad (0 \le z \le L) \quad (2)$$

where k_i is the LDF coefficient and $q_i^*(c_\mathrm{A}, c_\mathrm{B})$ is the adsorption isotherm of component i, which relates its equilibrium concentration in the adsorbed phase (q_i^*) with the solute concentrations (c_A and c_B) in the bulk fluid.

Equation 1 is subjected to the following boundary conditions

$$c_{ij} - \frac{D_{ij}}{v_j} \frac{\partial c_{ij}}{\partial z} = c_{ij}^{\mathrm{in}} \qquad \text{for } z = 0 \quad (3)$$

$$\frac{\partial c_{ij}}{\partial z} = 0 \qquad \text{for } z = L \quad (4)$$

where c_{ij}^{in} is the concentration of solute i at the inlet of the jth column. This concentration is determined by the solute material balance at the node between columns $j - 1$ and j, which can be expressed as

$$c_{ij}^{\mathrm{in}} = \alpha_j c_{i,j-1}^{\mathrm{out}} + (1 - \alpha_j) c_{ij}^{\mathrm{ex}} \qquad \alpha_j = \frac{\min\{v_{j-1}, v_j\}}{v_j} \quad (5)$$

where $c_{i,j-1}^{\mathrm{out}}$ is shorthand for the concentration $c_{i,j-1}(L, t)$ at the outlet of column $j - 1$ and c_{ij}^{ex} is the concentration of an external inlet stream (either eluent or feed), if the corresponding port is opened. The nodes can be classified according to the sign of $v_j - v_{j-1}$:

- Connecting node: $v_j = v_{j-1}$ ($\alpha_j = 1$)
- Eluent node: $v_j > v_{j-1}$ ($\alpha_j = v_{j-1}/v_j$), $c_{ij}^{\mathrm{ex}} = 0$
- Feed node: $v_j > v_{j-1}$ ($\alpha_j = v_{j-1}/v_j$), $c_{ij}^{\mathrm{ex}} = c_i^{\mathrm{F}}$, where c_i^{F} is the feed concentration
- Extract and raffinate nodes: $v_j < v_{j-1}$ ($\alpha_j = 1$)

Notice that if the feed and eluent ports between columns $j - 1$ and j are closed (that is, $v_j < v_{j-1}$), Eq. 5 correctly ignores the value of c_{ij}^{ex} because $\alpha_j = 1$, which eliminates the second term on the right-hand side of the equation.

The cyclic operation of the SMB with port configuration $N_\mathrm{I}/N_\mathrm{II}/N_\mathrm{III}/N_\mathrm{IV}$ ($N = \sum_{k=\mathrm{I}}^{\mathrm{IV}} N_k$), that is, N_I columns in section I, N_II columns in section II, and so forth, is defined by imposing the following time-periodic conditions on v_j and c_{ij}^{ex}

$$v_j(t) = \begin{cases} v_\mathrm{I} & 0 \le n_j < N_\mathrm{I} \\ v_\mathrm{IV} & N_\mathrm{I} \le n_j < N_\mathrm{I} + N_\mathrm{IV} \\ v_\mathrm{III} & N_\mathrm{I} + N_\mathrm{IV} \le n_j < N - N_\mathrm{II} \\ v_\mathrm{II} & N - N_\mathrm{II} \le n_j < N \end{cases} \quad (6)$$

$$c_{ij}^{\mathrm{ex}}(t) = \begin{cases} c_i^{\mathrm{E}} & N_\mathrm{I} - 1 \le n_j < N_\mathrm{I} \\ c_i^{\mathrm{F}} & N - N_\mathrm{II} - 1 \le n_j < N - N_\mathrm{II} \\ 0 & \text{otherwise} \end{cases} \quad (7)$$

Here, τ is the switching time (that is, the time span between the switching of port locations) and n_j is defined as

$$n_j = [t/\tau + (N + 1 - j)] \bmod N \qquad a \bmod b \equiv a - b\,\mathrm{int}(a/b) \quad (8)$$

and $v_\mathrm{I}, \ldots, v_\mathrm{IV}$ are the interstitial velocities in each of the four sections. These obey the global node balances

$$v_\mathrm{I} = v_\mathrm{IV} + Q_\mathrm{E}/(A\varepsilon) \quad (9)$$

$$v_\mathrm{II} = v_\mathrm{I} - Q_\mathrm{X}/(A\varepsilon) \quad (10)$$

$$v_\mathrm{III} = v_\mathrm{II} + Q_\mathrm{F}/(A\varepsilon) \quad (11)$$

$$v_\mathrm{IV} = v_\mathrm{III} - Q_\mathrm{R}/(A\varepsilon) \quad (12)$$

where A is the cross-sectional area of the columns and the Q values are the inlet/outlet flow rates: eluent (Q_E), extract (Q_X), feed (Q_F), and raffinate (Q_R). Because the system has N columns, the duration of the overall cycle (that is, the time required for each inlet/outlet line to recover its initial position) is $N\tau$.

If the inputs $v_j(t)$ and $c_{ij}^{\mathrm{ex}}(t)$ are constant or time-periodic of period τ, the process converges asymptotically toward a cyclic steady-state (CSS) regime. The definition of the CSS regime depends on the frame of reference. If the observer is stationary, each column is identified according to its fixed position within the unit (or its index number j). In this case, the CSS condition is

$$c_{ij}(z, t + N\tau) = c_{ij}(z, t) \qquad q_{ij}(z, t + N\tau) = q_{ij}(z, t) \qquad (0 \le z \le L) \quad (13)$$

which states that the spatially distributed concentration profiles at the beginning and at the end of the cycle must be identical.

If the frame of reference moves with the inlet/outlet lines, the CSS condition can be expressed as

$$c_{i,j+1}(z, t + \tau) = c_{ij}(z, t) \qquad q_{i,j+1}(z, t + \tau) = q_{ij}(z, t) \qquad (0 \le z \le L) \quad (14)$$

Equation 14 provides an alternative definition of the CSS for a standard SMB process: the spatially distributed concentration profiles at the start and at the end of a switching period are identical, apart from a shift of exactly one column. Equation 14 is the basis for a method of directly calculating the CSS regime.[23]

The mathematical basis of the SMB process reviewed above establishes the theoretical framework for developing an analogous single-column chromatographic system. At first glance this seems to be a nontrivial exercise. The solution, however, is rather simple as is shown next.

It is convenient to first tackle the problem from a theoretical standpoint and then to discuss how the process model can be realized experimentally. Notice that the former task requires the development of a mathematical formulation to simulate the behavior of the SMB process using the governing equations of a single chromatographic column. The key to achieve this is noticing that the only equation that references more than one column simultaneously is the solute node balance given by Eq. 5, which besides column j also references column $j-1$. For a single-column process the references to "$j-1$" must be removed from that equation. This is achieved by resorting to the CSS conditions. Looking into past process time we can write

$$c_{i,j-1}^{\text{out}}(t) = c_{i,j-1}^{\text{out}}(t - N\tau) = c_{ij}^{\text{out}}(t - N\tau + \tau) \quad \text{(15)}$$

from Eq. 13 from Eq. 14

and using Eq. 6 for the velocity,

$$v_{j-1}(t) = v_j(t - N\tau + \tau) \quad \text{(16)}$$

Equations 15 and 16 may be used to rearrange Eq. 5 so that it references column j only. The resulting expression is

$$c_i^{\text{in}}(t) = \alpha c_i^{\text{out}}(t') + (1-\alpha)c_i^{\text{ex}}(t) \qquad \alpha = \frac{\min\{v(t'), v(t)\}}{v(t)}$$
$$t' = t - (N-1)\tau \quad \text{(17)}$$

where the time dependency is shown explicitly and, for simplicity, the j subscript is omitted because its value is fixed. The periodic conditions imposed on $v(t)$ and $c_i^{\text{ex}}(t)$ for the single-column model are defined by Eqs. 6 and 7, with j set to one of the integer values between 1 and N. The choice is arbitrary; one model with $j = j_1$ behaves similarly to another model with $j = j_2$, except that they are phased out in time one from the other by $|j_2 - j_1|\tau$. We choose $j = N_{\text{II}} + 2$ so that the column is fed at the start of each cycle. Note that in Eq. 17, c_i^{out} is the concentration that left the column $(N-1)\tau$ time units before, whereas in the node balance of the SMB model c_i^{out} is the outlet concentration from the preceding column at the current instant.

Figure 2 compares a complete operating cycle of the simplest four-zone SMB (the one with port configuration 1/1/1/1) with that of the equivalent single-column model. It is seen that the single-column model is obtained by selecting an arbitrary column (shaded area) of the SMB unit and following its operation over a complete cycle. The recycle streams from the other columns of the SMB are replaced by the recycle stream of the

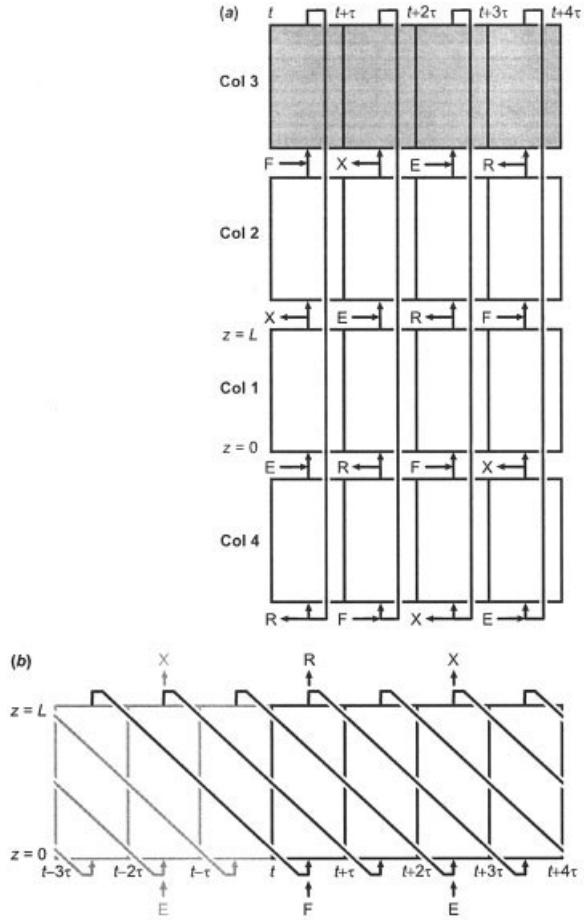

Figure 2. Operating cycle for (a) an SMB with port configuration 1/1/1/1 and (b) its equivalent single-column system with recycle lag.

The latter is obtained by selecting an arbitrary column of the SMB unit (such as column 3) and following its operation over a complete cycle (shaded area). The recycle streams from the other nonexistent SMB columns are mimicked by recycling, with a lag of $(N-1)\tau$ time units, the portion of the outlet stream of the column that is not withdrawn as product. The feed, eluent, extract, and raffinate streams are denoted by F, E, X, and R, respectively.

single-column at previous times. In essence, the single-column model can be characterized as follows:

- The part of its outlet stream that is not recovered as product is recycled to the column with a lag of $(N-1)\tau$ time units.
- It reproduces the periodic state of the SMB process because its node balance is obtained from the original SMB node balance by applying the CSS conditions.

The first point is the critical one from the perspective of process design, whereas the second one is precisely the necessary condition for the model to reproduce the behavior of the SMB. Under CSS conditions the two models cannot be discriminated, except for the discontinuous use of the inlet/outlet lines by the single-column model. Under these circumstances the SMB process is equivalent to N identical single-column processes operating in parallel with phase lags of τ time units. One important consequence of this result is that the use of four or more columns is not a necessary condition for simulating the

true moving bed process, unless continuous feed and product withdrawal is envisaged.

We end this section with a few notes regarding the use of the single-column model in the context of numerical simulation. First, the theoretical framework described here provides a competitive methodology for calculating the CSS by dynamic simulation. The CSS is established by starting from a given initial condition in the column and simulating the process operation over a sufficiently large number of cycles. However, as opposed to the traditional approach of integrating the equations for all columns, we integrate the equations for just one column and store the outlet concentrations at discrete times in a circular buffer, which is used to implement the recycle lag. The recycle is reconstructed from the discrete data stored in the buffer using a suitable scheme for data interpolation.

Second, it should be noted that the alternative of applying the CSS conditions forward in time was not explored here because that would not lead to a physically realizable process. From a numerical point of view, however, the resulting model with node balance given by

$$c_i^{\text{in}}(t) = \alpha c_i^{\text{out}}(t+\tau) + (1-\alpha)c_i^{\text{ex}}(t) \qquad \alpha = \frac{\min\{v(t+\tau),\, v(t)\}}{v(t)} \tag{18}$$

is the basis for an efficient method of directly computing the CSS. The method consists of discretizing the time coordinate for a single column over a complete cycle ($N\tau$ time units) and directly imposing the periodic boundary conditions given by Eq. 13. The resulting system of algebraic equations, obtained after discretization of the spatial coordinate, is solved directly to compute the CSS solution. Both methods are discussed in detail elsewhere.[24]

Practical Implementation of the Ideal Single-Column SMB Analog

System with perfectly mixed tanks

The one-column chromatographic system proposed by Abunasser et al.[15] is one way to implement in practice an approximation to the ideal single-column system described above. In their system several perfectly mixed tanks are coupled to the chromatographic column for collecting the portion of the outlet stream that is not withdrawn as product and for recycling it to the inlet of the column. The tanks are emptied in the order in which they were filled. This scheme allows for recycling in a manner that mimics the SMB behavior.

The complete cycle for the simplest one-column process developed by Abunasser et al.,[15] analogous to a four-column SMB, is shown in Figure 3. For this configuration the simplest analog has four tanks. Notice the striking resemblance between Figure 2b and Figure 3.

The process is well described elsewhere[15,16]; here, we add just a few notes regarding the analysis of the process and demonstrate that it is indeed an approximation to the ideal single-column process described above. Each tank cannot be filled or emptied in more than τ time units; otherwise, at least one tank would have to be filled and emptied at the same time. This rule sets a minimum number of N tanks for the system to work properly: $N-1$ tanks to collect the recycle stream during

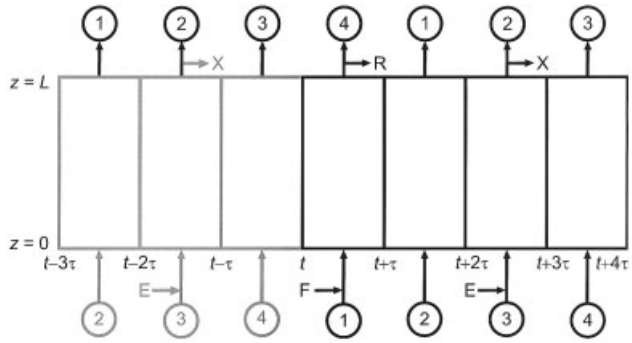

Figure 3. Complete operating cycle for the simplest version of the one-column process proposed by Abunasser et al.,[15] which approximates the operation of an SMB with port configuration 1/1/1/1.

In this configuration the analog has four tanks that replace the recycle streams shown in Figure 1b. The feed, eluent, extract, and raffinate streams are denoted by F, E, X, and R, respectively.

$(N-1)\tau$ time units (thereby creating the lag) to be subsequently inputted to the column, and one extra tank to prevent the overlap of filling and emptying operations on the same tank. At each instant, all tanks are filled except for two tanks: the one that is being filled with the portion of the outlet stream of the column that is not withdrawn as product and the other that is providing the recycle stream to the column. In any case, the total liquid volume in the N tanks gives the recycle volume collected during $(N-1)\tau$ time units.

For simplicity of analysis, let us assume that M_τ tanks are filled (emptied) during a switching interval and that the filling (emptying) time, $\tau_m = \tau/M_\tau$, is the same for all tanks. Notice that, although the tanks take the same time to fill (empty), they hold different amounts of liquid because they are filled (emptied) at different rates. Let us also assume that no tank is filled or emptied across a switching interval. These constraints render the analysis simpler but the conclusions hold for the more general case. Under the restrictions considered above, the total number of tanks required for the process to operate properly is $(N-1)M_\tau + 1$. This one-column analog is equivalent to replacing the node balance given by Eq. 17 with

$$c_i^{\text{in}}(t) = \alpha \tilde{c}_i(t) + (1-\alpha)c_i^{\text{ex}}(t) \tag{19}$$

where

$$\tilde{c}_i(t) = \frac{1}{\tau_m}\int_{t^*}^{t^*+\tau_m} c_i^{\text{out}}(v)dv \qquad t^* = \tau_m \text{int}(t/\tau_m) - (N-1)\tau \tag{20}$$

These equations show that the recycle of the ideal single-column system is replaced by a piecewise-constant approximation (staircase concentration profile) $\tilde{c}_i(t)$, where each concentration step is a consequence of the perfectly mixed contents of the tank being emptied. This is nicely exemplified in Figure 4, which compares typical temporal profiles of solute concentra-

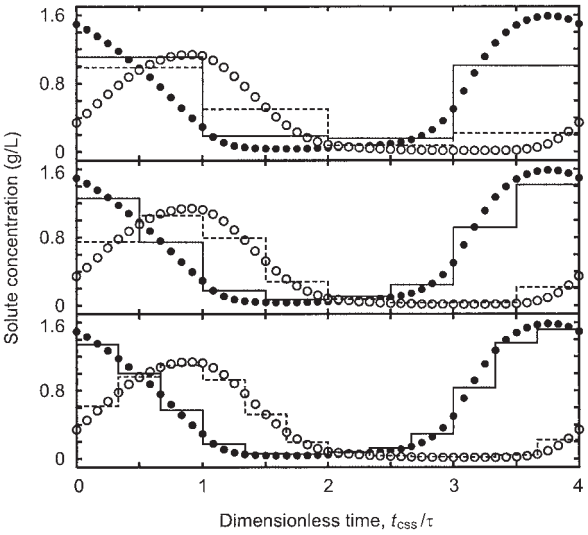

Figure 4. Comparison of the temporal profile of solute concentration in the recycle stream (symbols) that is inputted into the column of the ideal single-column model, that is, $c_i^{out}(t')$ in Eq. 17, with the corresponding concentration profile (lines) of the analog developed by Abunasser et al.[15] [that is, $\tilde{c}_i(t)$ in Eq. 19].

Both processes mimic the operation of a four-column SMB; the operating conditions and model parameters for the test case considered here are listed in Table 1 (solute A: ●, —; solute B: ○, – – –). The staircase shape of the lines results from the use of several tanks to implement the recycle lag. The number of tanks used by the analog in each plot is, from top to bottom: 4 ($M_\tau = 1$), 7 ($M_\tau = 2$), and 10 ($M_\tau = 3$). As the number of tanks is increased, the piecewise-constant concentration profile approaches the smooth concentration profile of the ideal single-column system.

tion in the recycle stream for the ideal single-column system and for three configurations of the equivalent analog using different number of tanks, when both processes are under CSS conditions. Notice that the concentration profiles of the ideal single-column process are identical to those of the SMB process being mimicked. The simplest analog configuration, the one with four tanks ($M_\tau = 1$), is shown in the top plot of Figure 4; each tank is filled during a complete switching interval ($\tau_m = \tau$). In the middle plot, the number of tanks has been increased to seven ($M_\tau = 2$, $\tau_m = \tau/2$) and in the bottom plot the number of tanks is ten ($M_\tau = 3$, $\tau_m = \tau/3$). Figure 4 shows that as the number of tanks is increased, the piecewise-constant concentration profile steadily approaches the profile of the ideal single-column system. From the definition of τ_m and Eq. 20 it is clear that

$$\lim_{M_\tau \to \infty} \tau_m = 0 \qquad \lim_{M_\tau \to \infty} \tilde{c}_i(t) = c_i^{out}(t') \qquad t' = t - (N-1)\tau \tag{21}$$

Equation 21 provides a formal proof that the analog of Wankat and coworkers[15,16] approaches the behavior of the SMB process as the number of tanks is increased. It is also clear that this conclusion holds for systems in which the filling time is not the same for all tanks or the charge/discharge of a tank crosses the boundary of a switching interval.

This one-column system is conceptually appealing, but can still be improved. Although the system uses a single chromatographic column, the ancillary equipment is not significantly reduced with respect to the analogous SMB. In its simplest configuration it needs at least four tanks, each requiring two valves (inlet and outlet), one relief valve, and probably other ancillary hardware. With respect to the equivalent SMB unit, three chromatographic columns have been replaced by four tanks and the number of two-way valves has been reduced by half. However, the biggest drawback is that the purities achieved with the analog are lower than those with the SMB for the same productivity and desorbent-to-feed, Q_E/Q_F, values. This is because of the loss of separation attributed to mixing in the tanks, which can be circumvented only by increasing the Q_E/Q_F value or by dividing the tanks into several smaller ones. The former option increases the separation cost, whereas the latter increases the bulkiness and capital cost of the unit.

New system with plug-flow recycle

Our single-column chromatographic process is more elegant and simpler to implement. Its main strength is that, in principle, it can achieve the same purities as those of the SMB. The basis for our process is that a recycle lag can be implemented in practice by a plug-flow device with a mean residence time equal to the time lag. This is equivalent to replacing the node balance given by Eq. 17 with

$$c_i^{in}(t) = \alpha \tilde{c}_i(1, t) + (1 - \alpha) c_i^{ex}(t) \tag{22}$$

where $\tilde{c}_i(x, t)$ is now a spatially distributed concentration that satisfies the plug-flow equation

$$\frac{\partial \tilde{c}_i}{\partial t} + \frac{1}{(N-1)\tau} \frac{\partial \tilde{c}_i}{\partial x} = 0 \qquad (0 < x \leq 1) \tag{23}$$

subjected to the inlet boundary condition

$$\tilde{c}_i(0, t) = c_i^{out}(t) \tag{24}$$

Unfortunately, this simple scheme is still not a practical solution because Eq. 23 assumes that the fluid is fed and withdrawn from the plug-flow device at the same rate. This is not the case for the ideal single-column system, where the flow rate of the portion of the outlet stream of the column for recycling and that of the recycled stream are different during some steps of the cycle. This happens because the recycle lag is not a multiple of the overall cycle duration $N\tau$.

To solve this problem a more ingenious setup[1] is needed, which is illustrated in Figure 5. The schematic shows the configuration of our single-column system that is analogous to a four-column SMB. The chromatographic column is connected in loop to a plug-flow tube, which has a spring-actuating piston at one end. The spring is continuously pushing the piston against the fluid. The movement of the piston compensates for

[1] Patent pending.

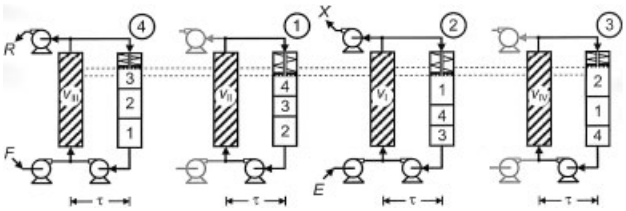

Figure 5. Single-column chromatographic process with recycle lag proposed in this work analogous to a four-zone SMB.

The chromatographic column is connected to a plug-flow tube with a piston at one end. The tube implements a recycle lag of $(N-1)\tau$ time units. The movement of the piston compensates for the difference in flow rates at the inlet and outlet of the tube that occur during some steps of the cycle. The complete cycle depicted here is for the configuration equivalent to a four-column SMB unit. The feed, eluent, extract, and raffinate streams are denoted by *F*, *E*, *X*, and *R*, respectively.

the difference between the inlet and outlet flow rates. The tube has internal elements, or packing, to break up the velocity distortion (Poiseuille flow), arising from the no-slip condition of the fluid at the tube wall, and to provide a flow that is as close as possible to plug flow. There are several options to achieve this, such as structured or random inert packing with large void fraction, or corrugated walls. A prototype apparatus is being built to determine the effectiveness of several alternatives. Here, we focus on the conceptual implementation of the process and defer its experimental validation to a subsequent study.

Both the piston placement and pump arrangement shown in the schematic diagram of Figure 5 are not mandatory; the piston can be set opposite to the direction of fluid flow and the recycle pump can be placed at the outlet of the chromatographic column. However, by placing the recycle pump as shown in Figure 5 the recycle tube works at the lowest pressure in the system, whereas the highest pressure value is at the recycle pump outlet. In this configuration the force exerted by the spring is minimized. The use of three pumps provides the easiest implementation. An alternative setup, which saves one pump, replaces the product withdrawal pump by a ratio-control system that includes a flow meter, a control valve, and a flow-rate controller.

The operation of the single-column process shown in Figure 5 deserves a closer look. During the first switching interval of a cycle the column is operating as if it were in section III of the equivalent SMB. The recycle stream is pumped from the tube with flow rate $Q_{II} = \varepsilon v_{II} A_c$ (where A_c is the cross-sectional area of the chromatographic column) is mixed with the feed and inputted to the column with interstitial velocity v_{III}. Part of the outlet stream of the column is collected as raffinate with flow rate $Q_R = \varepsilon(v_{III} - v_{IV})A_c$, the rest is fed to the recycle tube with flow rate $Q_{IV} = \varepsilon v_{IV} A_c$. Given that $Q_{II} > Q_{IV}$, the piston expands to compensate for the reduction of liquid in the recycle tube.

During the second and fourth switching intervals the chromatographic column is, respectively, in section II and section IV of the equivalent SMB system. In both cases the separation unit operates in closed loop with liquid being fed and withdrawn from the recycle tube at the same rate. The piston is stationary during both switching intervals.

During the third switching interval the column is in section I; part of its outlet stream is withdrawn as product (extract) with flow rate $Q_X = \varepsilon(v_I - v_{II})A_c$ and the rest is fed to the recycle tube with flow rate Q_{II}. Liquid is pumped from the recycle tube with flow rate Q_{IV}, diluted with fresh eluent, and fed to the column with interstitial velocity v_I. Because $Q_{II} > Q_{IV}$, the piston contracts to accommodate the extra liquid that is being accumulated in the recycle tube.

Figure 6 shows the schematic of a complete cycle for the proposed single-column process with configuration analogous to a four-zone SMB unit with two columns per zone (2/2/2/2). The cycle is more complex than that in Figure 5 because it is divided into more steps (the number of columns in the equivalent SMB has doubled and the switching interval has halved), although the operating principle is similar. The piston now has four stop positions (denoted A–D in Figure 6), instead of the previous two, and there are two pairs of consecutive switching intervals during which neither the inlet nor the outlet flow rates of the recycle tube vary. Each one of these pairs of switching intervals can be combined into a single one with twice the duration.

Many of the advantages of using a single-column system have been highlighted elsewhere.[15] The system is a simpler, more-flexible, and less-expensive alternative to the SMB process, which provides the same specific productivity, that is,

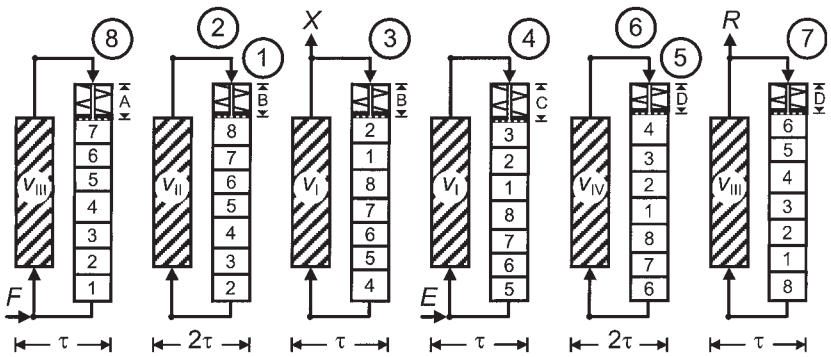

Figure 6. Schematic similar to that of Figure 5, but for the configuration equivalent to a 8-column SMB unit with port configuration 2/2/2/2.

Notice that the piston has more intermediate positions than in the scheme of Figure 5. The second and third switching intervals of each cycle can be lumped into a single step of duration 2τ; this is also applicable to the sixth and seventh switching intervals.

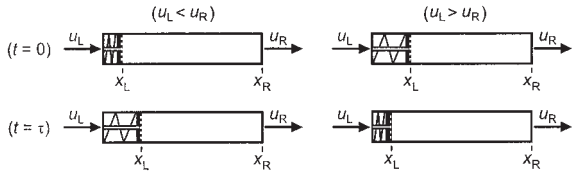

Figure 7. Piston movement. Liquid is fed to the recycle tube with velocity u_L and withdrawn with velocity u_R in the direction shown in the drawing.

The spring is constantly pushing the piston against the fluid. If the recycle pump is placed as shown in Figure 5, the tube is at the lowest pressure in the system and the piston can be designed so that the force exerted by the spring is minimum. x_R is fixed but x_L follows the piston as it moves. At each instant, the effective length of the tube is $x_R - x_L$. If $u_L < u_R$, the spring expands and x_L moves in the direction of x_R; the opposite happens when $u_L > u_R$.

$$\frac{\text{feed volume processed per cycle}}{\text{amount of stationary phase}} \tag{25}$$

Because the process uses a single column, the need to obtain adequate packing reproducibility on several columns is not an issue. Second, the total pressure drop is 1/*N*th that of the equivalent SMB process. This may be a big advantage if a particle size smaller than those appropriate for the equivalent SMB is used because it decreases the mass transfer resistance and allows for higher flow rates in the system. The specific productivity is thus increased. An added advantage is that the hydrodynamic contribution to band broadening in the chromatographic column is reduced because the Péclet number is increased.

The operation of the piston is shown schematically in Figure 7. Liquid is fed to the tube with inlet velocity u_L and withdrawn with outlet velocity u_R. The tube outlet is at a fixed distance x_R, whereas the inlet x_L moves with the piston, with velocity equal to $u_R - u_L$, arising from the difference between the inlet and outlet velocities. If $u_R > u_L$, the piston reduces the effective length ($x_R - x_L$) of the tube to compensate for the liquid volume that is withdrawn in excess to the feed value. If $u_R < u_L$, the spring contracts to create the necessary space for accommodating the excess liquid into the tube.

As a first approximation, the transport of solute through the recycle tube is described by an axially dispersed flow model, as follows:

$$\frac{\partial \tilde{c}_i}{\partial t} + u_R \frac{\partial \tilde{c}_i}{\partial x} - \tilde{D} \frac{\partial^2 \tilde{c}_i}{\partial x^2} = 0 \qquad (x_L < x \le x_R) \tag{26}$$

subjected to the boundary conditions

$$\tilde{c}_i = c_i^{\text{out}} \qquad \text{for } x = x_L \qquad \frac{dx_L}{dt} = u_R - u_L \tag{27}$$

$$\frac{\partial \tilde{c}_i}{\partial x} = 0 \qquad \text{for } x = x_R \tag{28}$$

Notice that Eq. 27 is a moving boundary condition. The dispersion coefficient $\tilde{D}$ accounts for the spread of the concentration profiles by the presence of molecular diffusion and velocity distortion (hydrodynamic dispersion) that is not fully eliminated by the internal elements of the tube.

We define a Péclet number ($\widetilde{\text{Pe}}$) for hydrodynamic dispersion in the tube, as

$$\widetilde{\text{Pe}} = \frac{u_R[x_R - x_L(0)]}{\tilde{D}} \tag{29}$$

Here, $\widetilde{\text{Pe}}$ is used as a general parameter to account for deviations from perfect plug flow in the tube, and to demonstrate the practical need for an efficient plug-flow device for the system to work correctly. In actual engineering work, $\widetilde{\text{Pe}}$ would be a sizing or design parameter. When designing a new unit, $\widetilde{\text{Pe}}$ would provide an estimate of the maximum admissible value of $\tilde{D}$ (which is directly related to the characteristics of the internal elements of the recycle tube) for product purity to be kept, within a given tolerance, near to that of the equivalent SMB. For an existing unit, $\widetilde{\text{Pe}}$ would be an extra parameter to be taken into account when determining the operating conditions (the appropriate flow rates for each step of the cycle) to obtain a desired separation performance. It should be pointed out that Eqs. 26–28 provide a reasonable description of the flow through random or structured inert packing, but may very well be inadequate to describe the impact of other types of internals on the flow field.

Equation 26 is easier to solve numerically if the moving boundary condition is replaced by a stationary one. To achieve this we introduce a change of variable that maps the spatial domain $x \in [x_L, x_R]$ onto a dimensionless domain $\xi \in [0, 1]$, of fixed length, through the transformation

$$\xi = (x - x_L)/(x_R - x_L) \tag{30}$$

Using the chain rule we obtain

$$\frac{\partial \tilde{c}_i(\xi, t)}{\partial t} = \frac{\partial \tilde{c}_i(x, t)}{\partial t} + \frac{\partial \tilde{c}_i(x, t)}{\partial x} \frac{\partial x(\xi, t)}{\partial t} \tag{31}$$

which allows us to rewrite Eqs. 26–28 as

$$\frac{\partial \tilde{c}_i}{\partial t} + \frac{\tilde{u}_R - (\tilde{u}_R - \tilde{u}_L)(1 - \xi)}{1 - (\tilde{u}_R - \tilde{u}_L)t} \frac{\partial \tilde{c}_i}{\partial \xi} - \frac{\tilde{u}_R/\widetilde{\text{Pe}}}{[1 - (\tilde{u}_R - \tilde{u}_L)t]^2} \frac{\partial^2 \tilde{c}_i}{\partial \xi^2} = 0 \qquad (0 < \xi \le 1) \tag{32}$$

$$\tilde{c}_i(0, t) = c_i^{\text{out}}(t) \qquad \left(\frac{\partial \tilde{c}_i}{\partial x}\right)_{x_R} = 0 \tag{33}$$

where $\tilde{u} = u/[x_R - x_L(0)]$. The convective term can also be rewritten in conservative form as

Table 2. Main Input Parameters for Each Step of a Full Cycle of the Proposed Single-Column Chromatographic Process*

Switching Interval	v	α	c_i^{ex}	$\tilde{u}_L\tau$	$\tilde{u}_R\tau$	c_i^R	c_i^X
1	v_{III}	$\frac{v_{II}}{v_{III}}$	c_i^F	$\frac{v_{IV}}{2v_{II}+v_{IV}}$	$\frac{v_{II}}{2v_{II}+v_{IV}}$	c_i^{out}	—
2	v_{II}	1	—	$\frac{v_{II}}{v_{II}+2v_{IV}}$	$\frac{v_{II}}{v_{II}+2v_{IV}}$	—	—
3	v_I	$\frac{v_{IV}}{v_I}$	c_i^E	$\frac{v_{II}}{v_{II}+2v_{IV}}$	$\frac{v_{IV}}{v_{II}+2v_{IV}}$	—	c_i^{out}
4	v_{IV}	1	—	$\frac{v_{IV}}{2v_{II}+v_{IV}}$	$\frac{v_{IV}}{2v_{II}+v_{IV}}$	—	—

*The configuration mimics the behavior of a four-section SMB with one column per section. The node balance is: $c_i^{in} = \alpha\tilde{c}_i^{out} + (1-\alpha)c_i^{ex}$.

$$\frac{\frac{\partial}{\partial\xi}\{[\tilde{u}_R-(\tilde{u}_R-\tilde{u}_L)(1-\xi)]\tilde{c}_i\}-(\tilde{u}_R-\tilde{u}_L)\tilde{c}_i}{1-(\tilde{u}_R-\tilde{u}_L)t} \tag{34}$$

Notice that $1/\tilde{u}_R$ is the average residence time of a fluid particle in the tube if its length is fixed at $x_R - x_L(0)$. Details of the numerical method for solving these equations, and its validation, are given in the appendix.

It is straightforward to determine the amount of liquid in the recycle tube, or its effective length, at the beginning of a given step of the cycle. Each slice of liquid, indexed in both Figures 5 and 6, is fed to the recycle tube and withdrawn from it with the same velocity, although it will travel along the tube with varying velocity as the steps change. Because a slice of liquid, say the jth one, is fed and withdrawn in τ time units, its volume is $u^{(j)}A_t\tau$, where $u^{(j)}$ is its feed velocity and A_t is the cross-sectional area of the tube; the length of tube taken by that slice of fluid is simply $u^{(j)}\tau$. Thus, the effective length of the tube at the beginning of the step in which slice j is inputted is

$$\tau\sum_{k=1,k\neq j}^{N}u^{(k)} \tag{35}$$

and the corresponding values of $\tilde{u}_L$ and $\tilde{u}_R$ are

$$\{\tilde{u}_L,\tilde{u}_R\}=\frac{\{u^{(j)},u^{(j+1)}\}}{\tau\sum_{k=1,k\neq j}^{N}u^{(k)}} \tag{36}$$

Because $\tilde{u}_L$ and $\tilde{u}_R$ are actually a ratio of u values, and each one of these is proportional to one of the interstitial velocities $v_I, \ldots, v_{IV}$, the ratio of the latter can be used instead. Table 2 lists the main input parameters governing each step of a full cycle of the proposed single-column process for a configuration analogous to a four-section SMB with one column per section; those for a configuration analogous to the SMB with two columns per section are listed in Table 3.

Figure 8 compares raffinate and extract purities for the single-column process proposed in this work, the SMB analog of Abunasser et al.,[15] and the equivalent four-section SMB. Note that the purities of the SMB are identical to those of the ideal single-column process described in the previous section, and are achieved by our process for $\widetilde{Pe}\to\infty$ and by the analog of Abunasser et al.[15] when $M_\tau\to\infty$. The analysis is carried out for three different port configurations: one column per section (1/1/1/1), six columns (1/2/2/1), and two columns per section (2/2/2/2).

The results show that, as the value of $\widetilde{Pe}$ is increased, the purities of our single-column process approach those of the equivalent SMB. The analog of Abunasser et al.[15] provides

Table 3. Main Input Parameters for Each Step of a Complete Cycle of the Proposed Single-Column Chromatographic Process*

Switching Interval	v	α	c_i^{ex}	$\tilde{u}_L\tau$	$\tilde{u}_R\tau$	c_i^R	c_i^X
1	v_{III}	$\frac{v_{II}}{v_{III}}$	c_i^F	$\frac{v_{III}}{v_I+3v_{II}+3v_{IV}}$	$\frac{v_{II}}{v_I+3v_{II}+3v_{IV}}$	—	—
2 and 3	v_{II}	1	—	$\frac{v_{II}}{v_I+2v_{II}+v_{III}+3v_{IV}}$	$\frac{v_{II}}{v_I+2v_{II}+v_{III}+3v_{IV}}$	—	—
4	v_I	1	—	$\frac{v_{II}}{v_I+2v_{II}+v_{III}+3v_{IV}}$	$\frac{v_I}{v_I+2v_{II}+v_{III}+3v_{IV}}$	c_i^{out}	—
5	v_I	$\frac{v_{IV}}{v_I}$	c_i^E	$\frac{v_I}{3v_{II}+v_{III}+3v_{IV}}$	$\frac{v_{IV}}{3v_{II}+v_{III}+3v_{IV}}$	—	—
6 and 7	v_{IV}	1	—	$\frac{v_{IV}}{v_I+3v_{II}+v_{III}+2v_{IV}}$	$\frac{v_{IV}}{v_I+3v_{II}+v_{III}+2v_{IV}}$	—	—
8	v_{III}	1	—	$\frac{v_{IV}}{v_I+3v_{II}+v_{III}+2v_{IV}}$	$\frac{v_{III}}{v_I+3v_{II}+v_{III}+2v_{IV}}$	—	c_i^{out}

*The configuration mimics the behavior of a four-section SMB with two columns per section. The node balance is: $c_i^{in} = \alpha\tilde{c}_i^{out} + (1-\alpha)c_i^{ex}$.

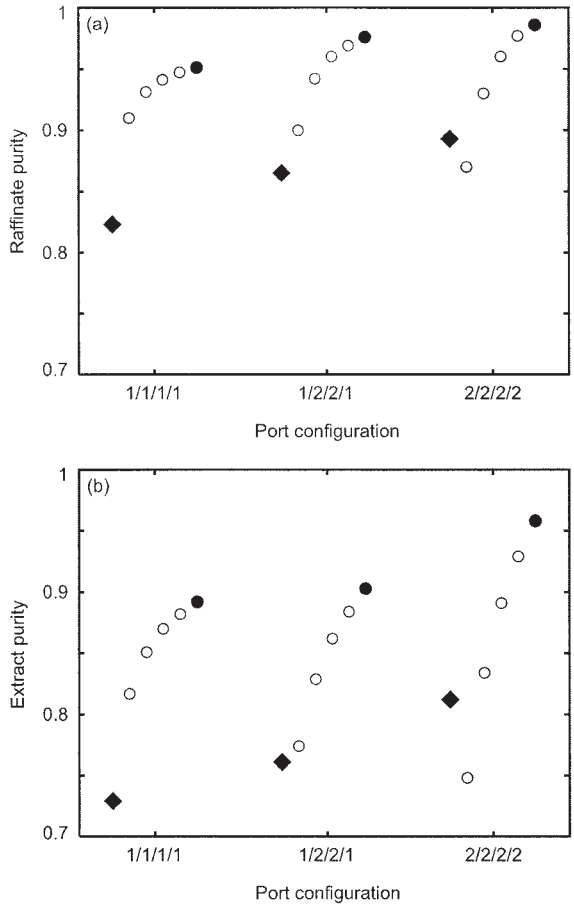

Figure 8. Comparison of raffinate (a) and extract (b) purities for our single-column process (○; the value of $\widetilde{\mathrm{Pe}}$ is, from left to right, 500, 1000, 2000, and 5000), the analog of Abunasser et al. [15] (♦), and the equivalent four-section SMB (●).

Note that the closed circles also denote purities for our single-column process when $\widetilde{\mathrm{Pe}} \rightarrow \infty$. The results are presented for three different port configurations: 1/1/1/1, 1/2/2/1, and 2/2/2/2. The operating conditions and model parameters for the test case considered here are listed in Table 1.

lower purities than our process for the range of $\widetilde{\mathrm{Pe}}$ values tested. The performance of their process improves with increasing number of columns of the analogous SMB. There are two reasons for this: the purities of the SMB are better when the sections are divided into more columns, but mostly because, as demonstrated in Figure 4, there is less loss of separation as a result of mixing in the tanks when their number is increased. This analysis is roughly equivalent to tracking the purities of our process by increasing both the number of columns of the analogous SMB and the value of $\widetilde{\mathrm{Pe}}$.

For a given configuration, the influence of $\widetilde{\mathrm{Pe}}$ on product purity is as expected, although the results are less obvious when different configurations are compared for the same $\widetilde{\mathrm{Pe}}$ value. For example, for $\widetilde{\mathrm{Pe}} = 500$ better purities are obtained with the configuration analogous to a four-column SMB than with the other two configurations. For $\widetilde{\mathrm{Pe}} = 1000$, the 1/2/2/1 configuration gives the best raffinate purity, whereas the highest extract purity is still obtained with the 1/1/1/1 configuration. For $\widetilde{\mathrm{Pe}} \geq 2000$, the purities follow the expected trend of improving with increasing number of columns of the equivalent SMB configuration. Thus, the impact of $\widetilde{\mathrm{Pe}}$ on product purity appears to be more severe when the number of columns of the analogous SMB configuration is larger. It should be pointed out that the results presented here are for a fixed set of operating conditions. No attempt was made to adjust the flow rates to optimize the separation performance for each $\widetilde{\mathrm{Pe}}$ value. Note also that the results have some embedded numerical diffusion, an inevitability of every spatial discretization scheme, that increases the value of the simulated Péclet number.

Figures 9–12 provide some insight into the mechanism by which $\widetilde{\mathrm{Pe}}$ influences product purity. The first two figures show the spatial profiles of solute concentration in the liquid phase that would be observed over the four sections of the SMB

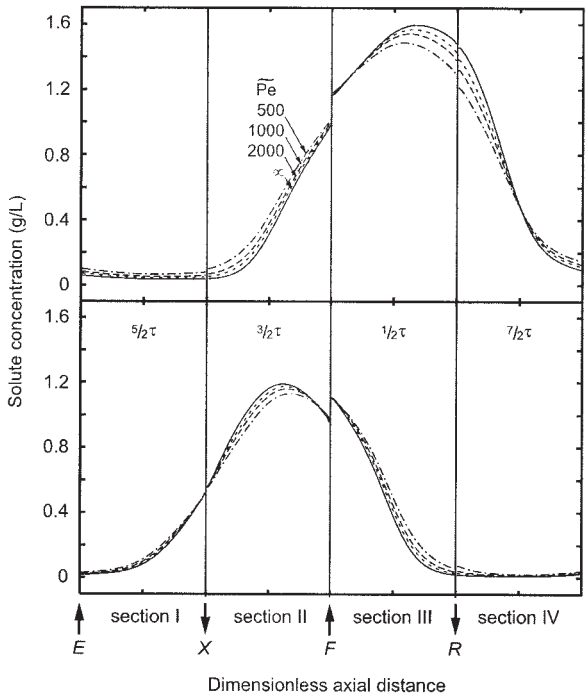

Figure 9. Spatial concentration profiles of less-retained (top plot) and more-retained component (bottom plot) in the middle of a switching interval, for the proposed single-column process analogous to a four-section SMB with one column per section.

The results are given for various values of the hydrodynamic Péclet number in the recycle tube, $\widetilde{\mathrm{Pe}}$, and were obtained after the process attained CSS conditions. Note that the results obtained for $\widetilde{\mathrm{Pe}} \rightarrow \infty$ are identical to those of the ideal single-column process and reproduce those of the equivalent SMB. To construct the spatial concentration profile spanning the four sections of the equivalent SMB, four snapshots of the profile in the column were taken with a sampling period equal to τ (as indicated in the graphic). The operating conditions and model parameters for the test case considered here are listed in Table 1.

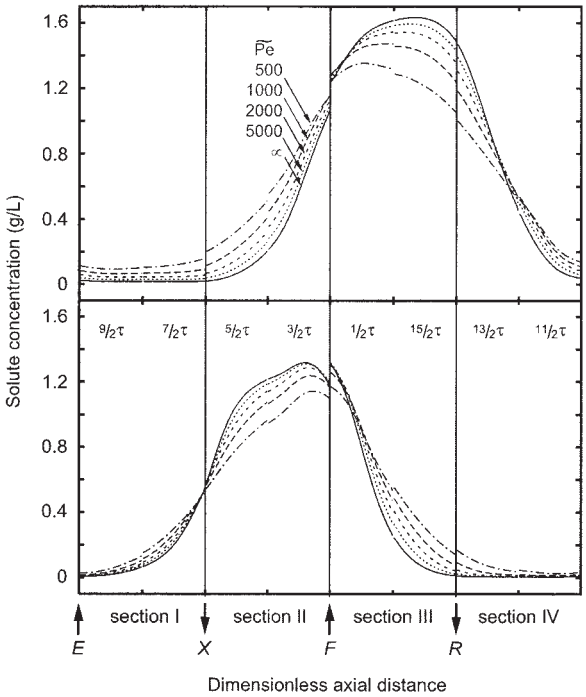

Figure 10. Plot similar to that of Figure 9, but for a configuration analogous to a four-section SMB with two columns per section.

Notice that the number of snapshots of the spatial concentration profile required to construct the profile spanning the four sections of the equivalent SMB has doubled.

mimicked by the single-column process. Figure 9 is for the analog to the SMB with one column per section, whereas Figure 10 is for the analog to the SMB with two columns per section. The data plotted in both figures were obtained after the system attained cyclic steady state. To construct each spatial concentration profile, we took several snapshots of the profile in the column of the analog with a sampling period equal to τ (as indicated in the respective graphic) and then plotted them sequentially. For a given $\widetilde{\text{Pe}}$ value, band broadening is more pronounced for the eight-column analog than that for the four-column analog. Dispersion tends to reduce solute concentration where it is higher and increase it where it is lower. This has a double-negative effect on product purity because it decreases the concentration of the target solute near its withdrawal point and increases that of the impurity. Because the spatial concentration profile is bell shaped and is constrained by the global material balance, it crosses another profile for a different $\widetilde{\text{Pe}}$ value twice along the four sections. For the less-retained component this happens near the feed point and halfway in section IV. The profiles for the more retained component cross others near the extract and feed points.

Figures 11 and 12 show temporal profiles of solute concentration at the outlet of the chromatographic column under CSS conditions for the two configurations analyzed in Figures 9 and 10. Again, it is seen that small values of $\widetilde{\text{Pe}}$ smooth the solute concentration profile, diluting it where it is higher and increasing its polluting effect where it is lower. Overall, these results demonstrate the practical need for an efficient plug-flow device for the system to work efficiently.

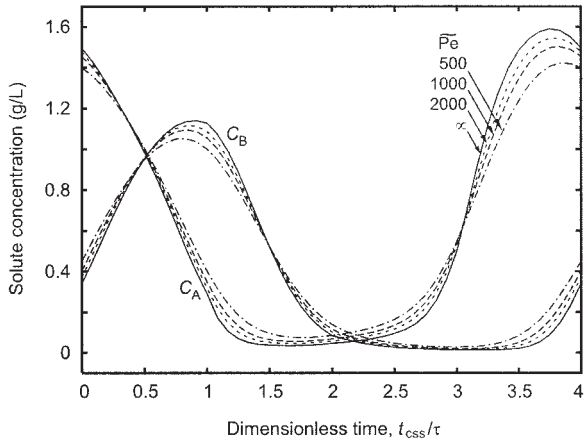

Figure 11. Temporal profiles of solute concentration at the outlet of the proposed single-column process for a configuration analogous to a four-section SMB with one column per section.

The results are given for various values of the hydrodynamic Péclet number in the recycle tube, $\widetilde{\text{Pe}}$, and were obtained after the process attained CSS conditions. Note that the results obtained for $\widetilde{\text{Pe}} \to \infty$ are identical to those of the ideal single-column process and reproduce those of the equivalent SMB. The operating conditions and model parameters for the test case considered here are listed in Table 1.

Conclusions

In this work we have demonstrated that the periodic state of the SMB can be reproduced by a single-column chromatographic process with a recycle lag of $(N - 1)\tau$ time units. To implement the recycle lag in practice, a special type of plug-flow tube has been designed. It includes internal elements to provide a flow that is as close as possible to plug flow, and a piston to compensate for the difference between the inlet and outlet flow rates. This is necessary because the recycle lag is not a multiple of the overall cycle duration. Our system is a more-compact, less-expensive, and simpler-to-operate alternative to the SMB that can potentially achieve the same purities while keeping the specific productivity constant.

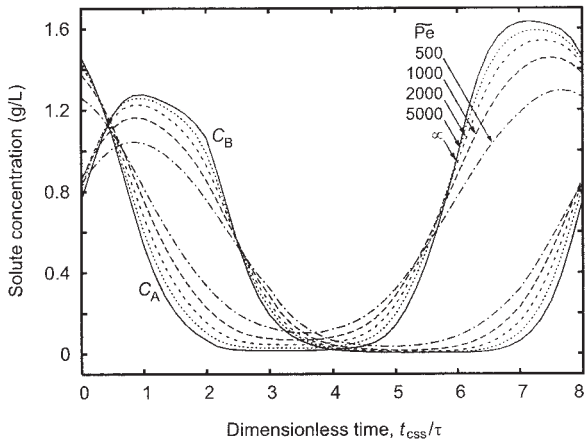

Figure 12. Plot similar to that of Figure 11, but for a configuration analogous to a four-section SMB with two columns per section.

It is clear that our single-column chromatographic process can be easily applied to other SMB configurations besides those considered in this work (such as three-zone arrangements). The numerous possibilities for improving SMB performance, through variation of parameters during a switching interval, are readily applicable to our single-column analog. For example, we have already obtained encouraging results by porting the VARICOL® concept[6] to our system. These recently developed novel cycles add extra flexibility to our process and the improved performance obtained with them can compensate for a less-perfect operation of the recycle tube. A detailed analysis of the application of these novel cyclic operation policies to our single-column process is the objective of future work.

Acknowledgments

Support from FCT/MCES (Portugal), through project No. POCTI/EQU/39391/2001 and PhD Grant SFRH/BD/13721/2003, is gratefully acknowledged. We are grateful to N. Abunasser and P. Wankat (Purdue University) for providing us with preprints of some of their papers.

Literature Cited

1. Juza M, Mazzotti M, Morbidelli M. Simulated moving bed chromatography and its application to chirotechnology. *Trends Biotechnol*. 2000;18:108.
2. Nicoud RM. The simulated moving bed: a powerful chromatographic process. *LC-GC*. 1992;5:43.
3. Jupke A, Epping A, Schmidt-Straub H. Optimal design of batch and simulated moving bed chromatographic separation processes. *J Chromatogr A*. 2002;944:93.
4. Strube J, Haumreisser S, Schmidt-Traub H, Schulte M, Ditz R. Comparison of batch elution and continuous simulated moving bed chromatography. *Org Proc Res Dev*. 1998;2:305.
5. Wankat PC. *Rate-Controlled Separations*. Amsterdam: Kluwer; 1990.
6. Ludemann-Hombourger O, Nicoud RM, Bailly M. The VARICOL process: A new multicolumn continuous chromatographic process. *Sep Sci Technol*. 2000;35:1829.
7. Antos D, Seidel-Morgenstern A. Application of gradients in the simulated moving bed process. *Chem Eng Sci*. 2001;56:6667.
8. Zang Y, Wankat PC. SMB operation strategy-partial feed. *Ind Eng Chem Res*. 2002;41:2504.
9. Zhang Z, Mazzotti M, Morbidelli M. PowerFeed operation of simulated moving bed units: Changing flow-rates during the switching interval. *J Chromatogr A*. 2003;1006:87.
10. Schramm H, Kienle A, Kaspereit M, Seidel-Morgenstern A. Improved operation of simulated moving bed process through cyclic modulation of feed flow and feed concentration. *Chem Eng Sci*. 1003;58:5217.
11. Lehoucq S, Verhève D, Wouwer AV, Cavoy E. SMB enantioseparation: Process development, modeling, and operating conditions. *AIChE J*. 2000;46:247.
12. Nicoud RM, Majors RE. Simulated moving bed chromatography for preparative separations. *LC-GC*. 2000;18:680.
13. Pais LS, Rodrigues AE. Design of simulated moving bed and Varicol processes for preparative separations with a low number of columns. *J Chromatogr A*. 2003;1006:33.
14. Ludemann-Hombourger O, Bailly M, Nicoud RM. Design of a simulated moving bed: Optimal particle size of the stationary phase. *Sep Sci Technol*. 2000;35:1298.
15. Abunasser N, Wankat PC, Kim YS, Koo YM. One-column chromatograph with recycle analogous to a four-zone simulated moving bed. *Ind Eng Chem Res*. 2003;42:5268.
16. Abunasser N, Wankat PC. One-column chromatograph with recycle analogous to simulated moving bed adsorbers: Analysis and applications. *Ind Eng Chem Res*. 2004;43:5291.
17. Pais LS, Loureiro JM, Rodrigues AE. Chiral separation by SMB chromatography. *Sep Purif Technol*. 2000;20:67.
18. Pais LS, Loureiro JM, Rodrigues AE. Separation of 1,1′-bi-2-naphthol enantiomers by continuous chromatography in simulated moving bed. *Chem Eng Sci*. 1997;52:245.
19. Pais LS, Loureiro JM, Rodrigues AE. Modeling, simulation and operation of a simulated moving bed for continuous chromatographic separation of 1,1′-bi-2-naphthol enantiomers. *J Chromatogr A*. 1997; 769:25.
20. Ruthven DM, Ching CH. Counter-current and simulated counter-current adsorption separation processes. *Chem Eng Sci*. 1989;44:1011.
21. Migliorini C, Gentilini A, Mazzotti M, Morbidelli M. Design of simulated moving bed units under nonideal conditions. *Ind Eng Chem Res*. 1999;38:2400.
22. Ruthven DM, Ching CB. In: Ganetsos G, Barker PE, eds. *Preparative and Production Scale Chromatography*. New York, NY: Marcel Dekker; 1993:629.
23. Kloppenburg E, Gilles ED. A new concept for operating simulated moving-bed processes. *Chem Eng Technol*. 1990;22:10.
24. Mota JPB, Araújo JMM. Efficient methods for calculating the periodic state of simulated-moving-bed process. 2004.
25. Schiesser WE. *The Numerical Method of Lines*. New York, NY: Academic Press; 1991.
26. Patankar SV. *Numerical Heat Transfer and Fluid Flow*. New York, NY: McGraw-Hill; 1980.
27. Waterson NP, Deconinck H. A unified approach to the design and application of bounded higher-order convection schemes. In: Taylor C, Durbetaki P, eds. *Numerical Methods in Laminar and Turbulent Flow*. Swansea, UK: Pineridge Press; 1995:203.
28. Jarvis RB, Pantelides CC. DASOLV—A differential-algebraic equation solver. Technical report. London, UK: Center for Process Systems Engineering, Imperial College; 1992.
29. Barton PI, Pantelides CC. Modeling of combined discrete and continuous processes. *AIChE J*. 1994;40:966.
30. Oh M, Pantelides CC. A modeling and simulation language for combined lumped and distributed parameter systems. *Comp Chem Eng*. 1996;20:611.

Appendix

The purpose of this appendix is to briefly describe the numerical method employed to solve Eq. 32. We demonstrate the validity of Eq. 32 to describe the axially dispersed flow in the recycle tube, and adequacy of the numerical procedure, by solving some test problems for which the analytical solution is easily derived. Because the same basic flow mechanism is assumed to govern solute transport in the chromatographic column, it is not surprising that the same numerical method was used to solve the governing equations for the chromatographic column.

We use the method-of-lines approach[25] to solve the conservation equations. The control-volume method[26] is applied to the spatial domain to convert the partial differential equations into a large system of differential-algebraic equations (DAEs) to which an efficient DAE solver is applied. To prevent nonphysical oscillations of the solution, the convective terms were discretized by the van Leer harmonic flux-limited scheme, implemented in the form advocated by Waterson and Deconinck.[27] The chromatographic column and the recycle tube are divided into 50 and 200 equally sized control volumes, respectively. The resulting DAEs, together with additional constraints (node balance) introduced to characterize the interactions between submodels of the process, are solved using gPROMS (general PROcess Modeling System), a software package for the modeling and simulation of processes with combined discrete and continuous characteristics (Process Systems Enterprise, http://www.psenterprise.com). Inside gPROMS, the DAE system is integrated over time using the DASOLV code[28] with absolute and relative tolerances of 10^{-5}. We note that gPROMS also allows the direct modeling of systems described by partial differential equations; the numerical discretization is applied automatically to these equations, thus reducing them to DAEs. However, the package does not currently implement the control-volume method with flux-limited correction, which we favor over other discretization methods. More information on the package can be found elsewhere.[29,30]

In the first numerical experiment (Figure A1), we simulate the injection of a rectangular pulse of tracer at infinite Péclet number ($\widetilde{\mathrm{Pe}} = \infty$), under conditions where the outlet flow rate is twice that of the inlet ($\tilde{u}_R/\tilde{u}_L = 2$). In this case the piston reduces the effective length of the tube to compensate for the liquid that is withdrawn in excess to the feed value. Because the exit flow rate is twice that of the feed, the width of the outputted pulse is reduced to half that of the injected pulse (top plot of Figure A1). At dimensionless instant $\tilde{u}_R t = 0.9$ (bottom plot of Figure A1), the right side of the pulse is located at $\xi = (0.9 - 0.9/2)/(1 - 0.9/2) = 0.82$, and the left side is positioned at $\xi = [0.5/2 + (0.9 - 0.5) - 0.9/2]/(1 - 0.9/2)$. It is seen that there is good agreement between the numerical and analytical solutions, although the former introduces some numerical dispersion.

Figure A2 summarizes the results obtained in the second test, which simulates the dispersive transport at low Péclet number ($\widetilde{\mathrm{Pe}} = 500$) of a rectangular profile of tracer. Again, the flow rates are such that $\tilde{u}_R/\tilde{u}_L = 2$. Because at the initial instant the rectangular profile is fully contained within the tube, and sufficiently distant from the piston, its dispersive transport is not affected by the movement of the piston. Thus, the problem can be solved using Eq. 26 on a fixed grid and the results subsequently mapped onto the dimensionless coordinate ξ. The numerical solution obtained by this approach is in perfect agreement with the solution obtained by solving Eq. 32.

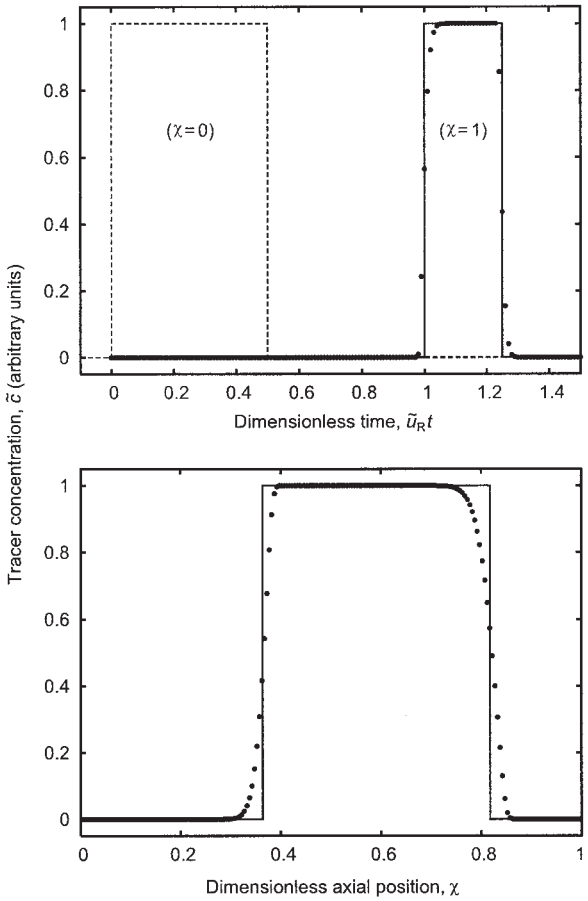

Figure A1. The first of a pair of numerical experiments to validate Eq. 32 and the numerical method for solving it.

This test simulates the injection of a rectangular pulse of tracer (dashed line) at infinite Péclet number (no hydrodynamic dispersion) under conditions where $\tilde{u}_R/\tilde{u}_L = 2$ (that is, liquid is withdrawn with flow rate that is twice that of the feed). The symbols are the numerical solution of the corresponding breakthrough curve (top plot) and spatial profile at dimensionless time $\tilde{u}_R t = 0.9$ (bottom plot); both are in very good agreement with the analytical solution (solid lines).

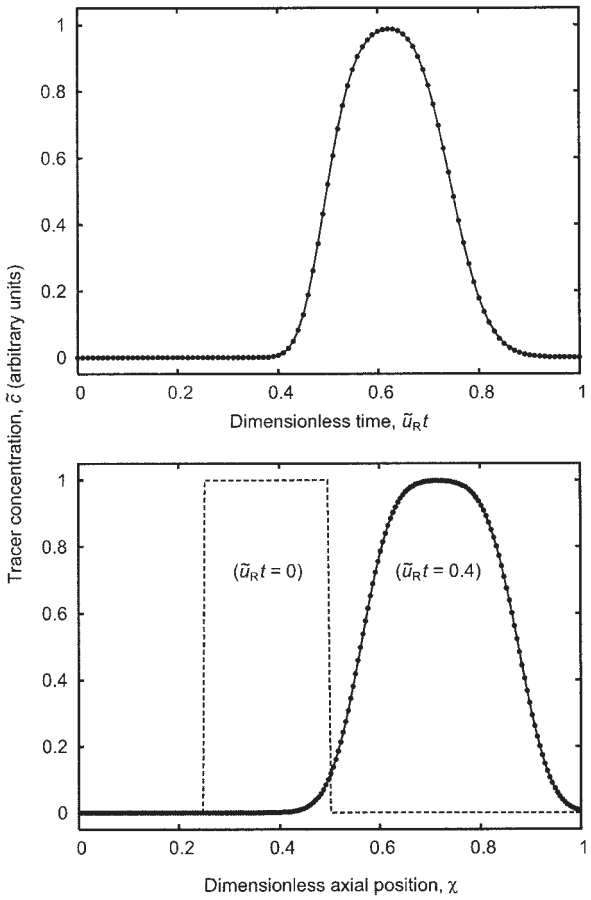

Figure A2. The second of a pair of numerical experiments to validate Eq. 32 and the numerical method for solving it.

This test simulates the dispersive transport ($\widetilde{\mathrm{Pe}} = 500$) of a rectangular profile of tracer (dashed line) initially contained within the tube. Again, the flow rates are such that $\tilde{u}_R/\tilde{u}_L = 2$. Because the inlet boundary condition for the tracer concentration is simply $\tilde{c}_i(0, t) = 0$, the problem can also be solved using Eq. 26 in a fixed grid provided that the internal tracer profile is adjusted to the true length of the tube. The symbols are the numerical solution of the corresponding breakthrough curve (bottom plot) and spatial profile at dimensionless time $\tilde{u}_R t = 0.4$ (top plot) using Eq. 32; both are in excellent agreement with the numerical solution of Eq. 26 obtained in a fixed grid (solid lines).

Manuscript received Aug. 25, 2004, and revision received Oct. 25, 2004.